Diamond & Related Materials 19 (2010) 324–328

Contents lists available at ScienceDirect

Diamond & Related Materials

journal homepage: www.elsevier.com/locate/diamond

Termination of diamond surfaces with hydrogen, oxygen and fluorine using a small, simple plasma gun

M.C. Salvadori [a,*], W.W.R. Araújo [a], F.S. Teixeira [b], M. Cattani [a], A. Pasquarelli [c], E.M. Oks [d], I.G. Brown [e]

[a] Institute of Physics, University of São Paulo, São Paulo, C.P. 66318, CEP 05315-970, São Paulo, Brazil
[b] Polytechnic School, University of São Paulo, São Paulo, SP Brazil
[c] University of Ulm, Department of Electron Devices & Circuits, D-89069 Ulm, Germany
[d] High Current Electronics Institute, Russian Academy of Sciences, Tomsk 634055, Russia
[e] Lawrence Berkeley National Laboratory, 1 Cyclotron Road, Berkeley, California 94720, USA

ARTICLE INFO

Article history:
Received 10 May 2009
Received in revised form 25 November 2009
Accepted 4 January 2010
Available online 11 January 2010

Keywords:
Diamond
CVD
Surface terminations
Plasma bombardment
Ion bombardment

ABSTRACT

We have formed and characterized polycrystalline diamond films with surfaces having hydrogen terminations, oxygen terminations, or fluorine terminations, using a small, simple and novel plasma gun to bombard the diamond surface, formed by plasma assisted CVD in a prior step, with ions of the wanted terminating species. The potential differences between surface regions with different terminations were measured by Kelvin Force Microscopy (KFM). The highest potential occurred for oxygen termination regions and the lowest for fluorine. The potential difference between regions with oxygen terminations and hydrogen terminations was about 80 mV, and between regions with hydrogen terminations and fluorine terminations about 150 mV. Regions with different terminations were identified and imaged using the secondary electron signal provided by scanning electron microscopy (SEM), since this signal presents contrast for surfaces with different electrical properties. The wettability of the surfaces with different terminations was evaluated, measuring contact angles. The sample with oxygen termination was the most hydrophilic, with a contact angle of 75°; hydrogen-terminated regions with 83°, and fluorine regions 93°, the most hydrophobic sample.

1. Introduction

Diamond is an important material for a wide range of applications because of its excellent chemical, electrical, thermal and mechanical properties. The diamond surface can be modified by various techniques and the versatility thereby yet further expanded. It is known that hydrogen termination of diamond surface bonds gives rise to high *p*-type surface conductivity even in undoped diamond [1–3], and oxygen termination of surface bonds results in an insulating surface [4,5]. These diamond surface properties have been used to fabricate electronic devices [6,7]. Differences between diamond surfaces are not limited to different electrical conductivities, but include hydrophobicity and hydrophilicity, and negative and positive electron affinity. These variations are caused primarily by differences between the surface dipole moments of carbon/hydrogen and carbon/oxygen bonds [8]. Fluorine termination of diamond surfaces has been investigated also [9–14]; these surfaces are negatively charged and hydrophobic [9], providing potential applications in biosensor devices [15].

In the work described here we formed polycrystalline diamond films with surfaces having hydrogen termination, oxygen termination, or fluorine termination, using a small, simple, novel plasma gun to bombard the diamond surface, formed by plasma assisted CVD in a prior step, with ions of the wanted terminating species. The surface potential difference between regions with different terminations was measured by Kelvin Force Microscopy (KFM); this has been reported previously for the case of oxygen terminated surfaces but not for fluorine [16–18]. Secondary electron imaging from scanning electron microscopy (SEM) was used to identify regions with different terminations, since this signal shows contrast between surfaces with different electrical properties [19–21]. The wettability of surfaces with different terminations was evaluated by contact angle measurements. For SEM and KFM analysis, the diamond surfaces were lithographed and exposed to different kinds of plasma surface modification, creating adjacent regions with different surface terminations. Diamond surfaces with a single kind of termination were also produced for contact angle measurements.

2. Materials and methods

Polycrystalline diamond films were grown by microwave plasma assisted chemical vapor deposition (MPACVD). The facility has been described in detail elsewhere [22,23]. The parameters used for the

* Corresponding author. Tel.: +55 11 3091 6857; fax: +55 11 3091 6749.
E-mail address: mcsalva@if.usp.br (M.C. Salvadori).

0925-9635/$ – see front matter © 2010 Elsevier B.V. All rights reserved.
doi:10.1016/j.diamond.2010.01.002

diamond growth were 300 sccm hydrogen flow rate, 3 sccm methane flow rate, 3 sccm nitrogen flow rate, 50 Torr chamber pressure, 850 °C substrate temperature, and the growth time was 24 h. Nitrogen was added to the gas phase so as to obtain nanocrystalline diamond films; in the absence of nitrogen microcrystalline films are formed [24,25]. The substrate used for the deposition was *n*-type silicon (100) polished with diamond powder. An SEM image of a typical diamond film obtained in this way is shown in Fig. 1. Fig. 2 shows a typical Raman spectrum. The equipment used was a Renishaw Raman System 3000. The samples were irradiated with the 632.8 nm line of a He–Ne laser (Spectra Physics). Measurements were carried out under ambient conditions using back-scattering geometry. This Raman spectrum is typical of nanocrystalline diamond films, but the peak at around 1150 cm^{-1} is a possible indication of trans-polyacetylene [26,27]. To confirm the film characterization, X-ray diffraction was done and the results are shown in Fig. 3. We used a Rigaku diffractometer with power given by $I=20$ mA and $V=40$ kV, using CuK_α ($\lambda=0.15418$ nm) monochromatic radiation in Bragg–Brentano geometry step scanning mode with $\Delta 2\theta=0.05°$ and counting time of 30 s. The X-ray diffraction clearly shows that the film is nanocrystalline diamond. The spectrum shows the two characteristic peaks of diamond. Using the Debye–Scherrer formula, an average crystallite size of 19.2 nm was obtained [24,28].

The CVD growth process delivers diamond film with hydrogen-terminated surface bonds. This is because the hydrogen fraction in the plasma synthesis process is very high (94%), with just 3% nitrogen as a possible "surface contamination"; the remaining gas is methane (CH_4), composed of carbon (diamond precursor) and hydrogen.

To replace the hydrogen terminations with either oxygen or fluorine, the diamond substrate was subsequently exposed for several minutes to the plasma stream produced by a small hollow-cathode plasma gun that has been described in detail elsewhere [29] and which we summarize briefly here. Of the various ways in which a gaseous plasma can be produced, the hollow-cathode discharge [30–33] stands out for its economy of design and its simplicity. Our plasma generator is a small hollow-cathode device driven by a simple home-made power supply system. An outline drawing of the plasma source is shown in Fig. 4(a). The source is of ceramic, stainless steel, and aluminum construction, with a tungsten anode mesh. The plasma discharge occurs within the hollow-cathode region, with the grounded tungsten mesh serving as anode. Plasma is extruded from the source as a slowly diverging plasma stream, into which the substrate to be ion bombarded is placed. A "starting electrode" at the rear of the hollow-cathode region is helpful in initiating breakdown and establishing the plasma when the source is first switched on. Gas is fed to the source through a small diameter plastic tube using a needle valve to control the pressure. For the present work, the feed gas was either oxygen at a working pressure in the vacuum chamber of 2×10^{-4} Torr, or sulfur hexafluoride (SF_6) at a chamber pressure of 7.5×10^{-3} Torr. The diamond sample was positioned some distance from the plasma gun—15 mm for SF_6 and 120 mm for O_2, these distances chosen simply based on the visual appearance of the plasma stream. A photograph of the source with extruded plasma beam is shown in Fig. 4(b).

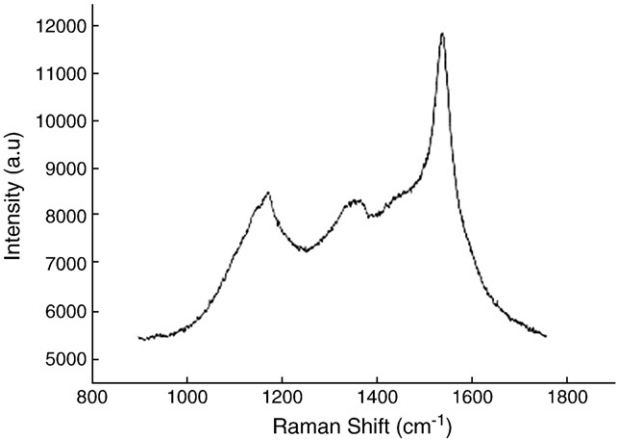

Fig. 2. Typical Raman spectrum of the diamond films used here.

Diamond surfaces with hydrogen, oxygen and fluorine terminations were imaged by Kelvin Force Microscopy (KFM) [16] to measure the potential differences between these regions. The equipment used was a NanoScope IIIA (Veeco, Santa Barbara, California). KFM is one of a number of possible operating modes of the Scanning Probe Microscope. Surface potential mapping was done using a two-pass system where the surface topography is obtained in the first pass and the surface potential is measured on the second pass. The two measurements are obtained one line at a time with both images displayed on the screen simultaneously. On the first pass, the sample topography is measured using standard intermittent contact mode (Tapping Mode); in this scan mode the cantilever is mechanically vibrated near its resonant frequency by a small piezoelectric element. On the second pass, the drive piezo that normally vibrates the cantilever is turned off, and instead, in order to measure the surface potential, an oscillating voltage is applied directly to the cantilever tip. If there is a DC voltage difference between the tip and sample, then there will be an oscillating electric force on the cantilever at frequency ω. This will cause the cantilever to vibrate, and the vibration amplitude can be detected. If the tip and sample are at the same DC voltage, there is no force on the cantilever at frequency ω and the cantilever amplitude will go to zero. The instrumentation determines the local surface potential by adjusting the DC voltage on the tip, V_{tip},

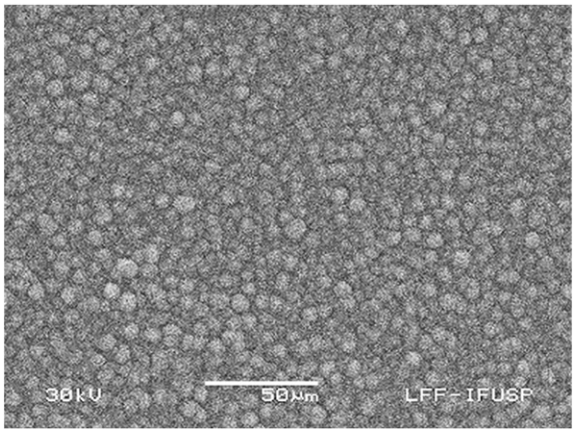

Fig. 1. Typical SEM image of the diamond films used in this work.

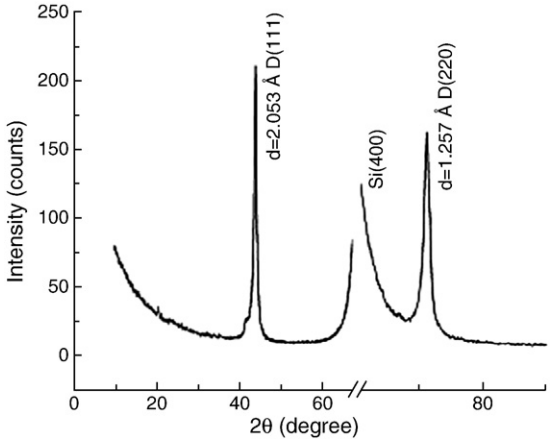

Fig. 3. Typical X-ray diffraction spectrum of the diamond films used here.

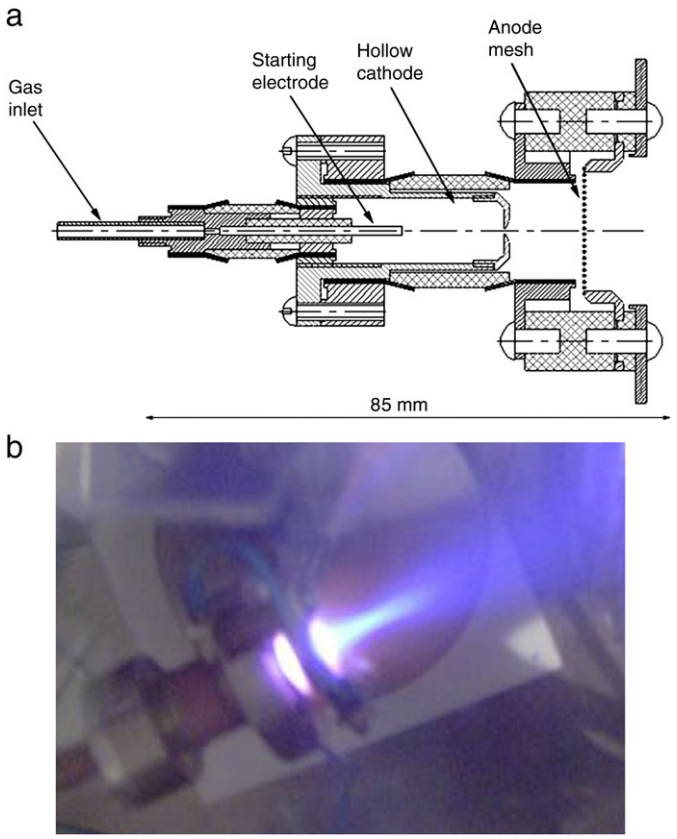

Fig. 4. Miniature hollow-cathode plasma gun. (a) Simplified schematic. (b) In operation, with extruded plasma stream.

until the oscillation amplitude goes to zero. At this point the tip voltage is the same as the surface potential. The voltage applied to the cantilever tip is recorded by the microscope to construct a voltage map of the surface. In this way, two images are obtained simultaneously: an atomic force microscopy (AFM) image and a KFM image, for exactly the same surface region.

Secondary electron images (by SEM) of the diamond surfaces with different terminations were used to identify the regions with different terminations [19–21]. The equipment used was a JEOL model JSM-6460 LV.

The wettability of the different surfaces was quantified using contact angle measurements. The sessile drop method was employed using deionized water. The equipment used for contact angle measurements was a KSV Modular CAM 200 System.

For KFM and SEM analysis it was necessary to create diamond surfaces with adjacent regions having different terminations. To produce these samples, the diamond surfaces were lithographed and exposed to different plasma processing. Three samples were prepared: the first sample with adjacent regions having hydrogen and oxygen terminations; a second sample with adjacent regions of hydrogen and fluorine terminations; and a third sample with hydrogen, fluorine and oxygen terminations. Initially three diamond film samples terminated with hydrogen were coated with PMMA (polymethylmethacrylate, a polymer used as a resist for electron beam lithography). Then a selected area of the PMMA was electron beam scanned in a SEM (JSM-6460 LV) using an e-beam nanolithography system (Nanometer Pattern Generation System—NPGS), creating a pattern. The samples were then immersed in a developing solution and rinsed in isopropyl alcohol. With this procedure, the region of the PMMA scanned by the electron beam was removed and the remaining area was preserved. All samples were then treated with plasma as described above, one sample using oxygen plasma and the other two samples using sulfur hexafluoride (SF_6) plasma. The remaining PMMA for all samples was removed in an acetone ultrasonic bath. Thus diamond samples with adjacent regions presenting hydrogen and oxygen terminations, and two samples with regions presenting hydrogen and fluorine terminations, were obtained. One of these last samples was again coated with PMMA, and a new selected area was electron beam scanned, creating another pattern. The sample was then immersed in developing solution, rinsed in isopropyl alcohol, and again treated with oxygen plasma and the remaining PMMA removed. Thus diamond samples with adjacent regions presenting terminations of hydrogen, fluorine and oxygen were obtained.

3. Results and discussion

AFM and KFM images of the diamond surface with adjacent regions having hydrogen and oxygen terminations are shown in Fig. 5. Fig. 5(a) is an AFM image and shows the film morphology. Fig. 5(b) is a KFM image; here the contrast represents the surface potential difference, with the lighter regions (higher potential) having oxygen terminations and the darker regions having hydrogen terminations. The *z*-scale in the KFM image relates quantitatively to the local potential difference between regions. Similar characterization was performed for a sample with regions presenting hydrogen and fluorine terminations, and for a third sample with adjacent regions presenting hydrogen, fluorine and oxygen terminations. AFM and the KFM images of this last sample are shown in Fig. 6(a) and (b), respectively. Here the lighter regions (higher potential) have oxygen terminations, the darker regions (lower potential) have

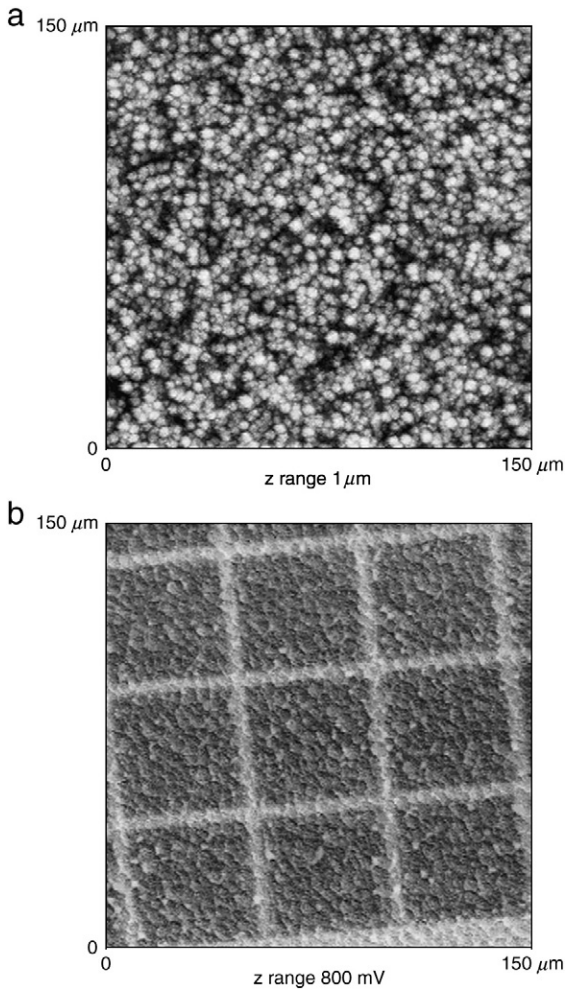

Fig. 5. (a) AFM, and (b) KFM images of diamond surface with adjacent regions having hydrogen and oxygen terminations. In the KFM image, the lighter regions correspond to oxygen terminations.

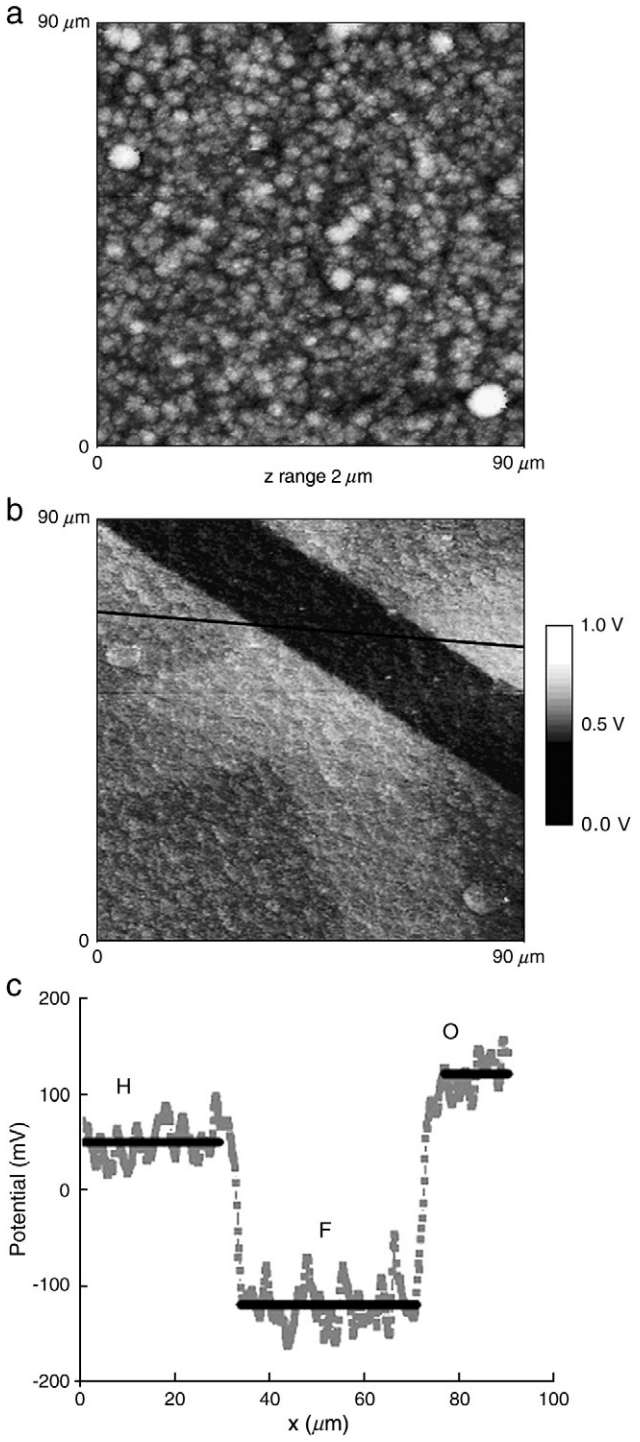

Fig. 6. (a) AFM, and (b) KFM images of diamond surface with adjacent regions having hydrogen, fluorine and oxygen terminations. The lightest regions are oxygen terminated, the intermediate regions hydrogen terminated, and the darkest regions are fluorine terminated. (c) Potential profile for the diamond surface; the profile was taken along the thin black line in the KFM image of Fig. 5(b). The *z*-scale to the right of the image relates the gray scale of the image to potential difference.

fluorine terminations, and the intermediate gray regions (intermediate potential) have hydrogen terminations. A typical potential profile for the diamond surface is shown in Fig. 6(c). The profile shown in this figure was taken along the thin black line shown in Fig. 6(b). The regions with oxygen termination have higher surface potential, the regions with fluorine termination have a lower potential, and the regions with hydrogen termination have an intermediate value. The measured potential difference between regions with oxygen terminations and

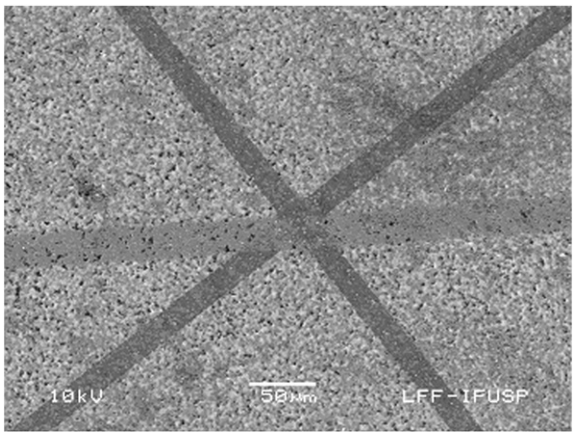

Fig. 7. Secondary electron images (SEM) of diamond surface with adjacent regions having hydrogen, fluorine and oxygen terminations. The image contrast is due to the different electrical properties of regions with different terminations.

hydrogen terminations was about 80 mV, and between regions with fluorine terminations and hydrogen terminations was about 150 mV. These results are consistent with measurements made with the other two samples. The potential difference measured for the sample shown in Fig. 5 (with oxygen terminations and hydrogen terminations) was about 95 mV, and for the sample with fluorine and hydrogen terminations about 165 mV. Preliminary experiments demonstrate that the potential difference between regions with different terminations depends on the plasma exposure time and the distance between the sample and the plasma source—i.e., on the total plasma flux incident on the surface.

Secondary electron images of diamond surfaces with different terminations were also obtained by SEM, as shown in Fig. 7. In this SEM image, the contrast is related to the surface terminations, and is not

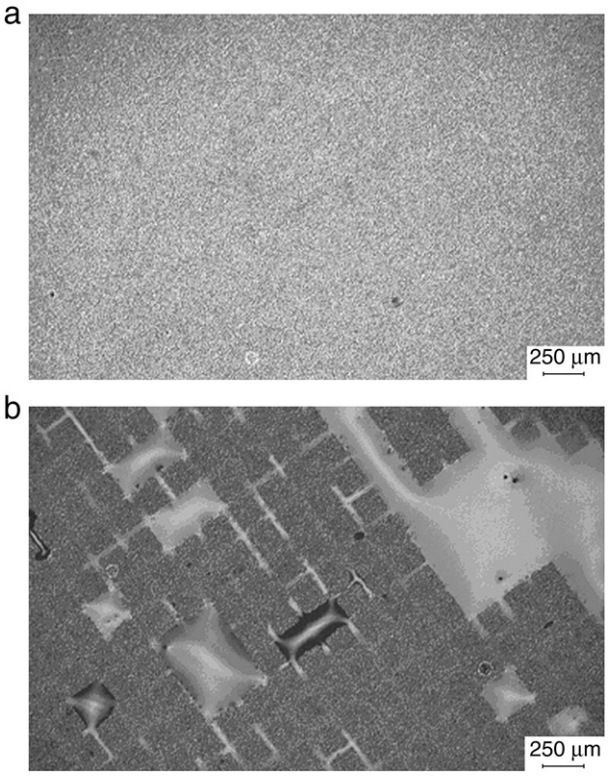

Fig. 8. Optical micrographs of diamond surfaces with adjacent regions having hydrogen and oxygen terminations. (a) Dry surface, showing no contrast between regions with different terminations; and (b) wet surface, showing clearly the hydrophilic regions, with oxygen terminations.

due to morphology as would be usual. The region with fluorine termination is the darker one, the region with hydrogen termination is the lighter one, and the third region is with oxygen termination. The contrast in this SEM image is due to the different electrical properties (secondary electron emission) generated by the different terminations.

Three more diamond surfaces were prepared for contact angle measurements. Each of these samples was produced with just one kind of termination. The first sample, with oxygen termination, showed a contact angle of 75°, the most hydrophilic sample; the second sample, with hydrogen termination, had a contact angle of 83°; and the third sample, with fluorine termination, 93°, the most hydrophobic sample. Fig. 8 shows optical micrographs of diamond surfaces with adjacent regions having hydrogen and oxygen terminations; Fig. 8(a) shows a dry surface and Fig. 8(b) a wet surface. The image of the dry surface has no contrast between the regions with different terminations. On the other hand, the image of the wet surface shows clearly the hydrophilic regions, with oxygen terminations.

4. Conclusion

Polycrystalline diamond thin films were formed by microwave plasma assisted CVD, and the surface carbon bonds terminated with either oxygen or fluorine by means of a small hollow-cathode plasma gun that subsequently was used to ion bombard the surface with the chosen ion species. Kelvin Force Microscopy allowed measurement of surface potential differences between regions with different terminations. The highest potential difference (with respect to the hydrogen-terminated region) was for oxygen termination, and the lowest for fluorine termination. The potential difference between regions with oxygen terminations and hydrogen terminations was about 150 mV, and between regions with fluorine and hydrogen terminations about 80 mV. Secondary electron imaging in scanning electron microscopy (SEM) was used to identify the regions with different terminations, since this signal shows contrast for surfaces with different electrical properties. The wettability of surfaces with different terminations was evaluated, yielding contact angles with pure water of 75° for oxygen terminated regions, 83° for hydrogen-terminated regions, and 93° for fluorine terminated regions.

Acknowledgments

This work was supported by the Fundação de Amparo a Pesquisa do Estado de São Paulo (FAPESP) and the Conselho Nacional de Desenvolvimento Científico e Tecnológico (CNPq), Brazil.

References

[1] M.I. Landstrass, K.V. Ravi, Appl. Phys. Lett. 55 (1989) 975.
[2] K. Hayashi, S. Yamanaka, H. Okushi, K. Kajimura, Appl. Phys. Lett. 68 (1996) 376.
[3] D. Takeuchi, M. Riedel, J. Ristein, L. Ley, Phys. Rev. B 68 (2003) 041304(R).
[4] J. Shirafuji, T. Sugino, Diamond Relat. Mater. 5 (1996) 706.
[5] M. Tachiki, T. Fukuda, K. Sugata, H. Seo, H. Umezawa, H. Kawarada, Appl. Surf. Sci. 159–160 (2000) 578.
[6] M. Tachiki, H. Seo, T. Banno, Y. Sumikawa, H. Umezawa, H. Kawarada, Appl. Phys. Lett. 81 (2002) 2854.
[7] H. Taniuchi, H. Umezawa, T. Arima, M. Tachiki, H. Kawarada, IEEE Electron Device Lett. 22 (2001) 390.
[8] H. Kawarada, Surf. Sci. Rep. 26 (1996) 205.
[9] S. Kuga, J.-H. Yang, H. Takahashi, K. Hirama, T. Iwasaki, H. Kawarada, J. Am. Chem. Soc. 130 (2008) 13251.
[10] M.A. Ray, T. Tyler, B. Hook, A. Martin, G. Cunningham, O. Shenderova, J.L. Davidson, M. Howell, W.P. Kang, G. McGuire, Diamond Relat. Mater. 16 (2007) 2087.
[11] C. Popov, W. Kulisch, S. Bliznakov, G. Ceccone, D. Gilliland, L. Sirghi, F. Rossi, Diamond Relat. Mater. 17 (2008) 1229.
[12] C.P. Kealey, T.M. Klapötke, D.W. McComb, M.I. Robertson, J.M. Winfield, J. Mater. Chem. 11 (2001) 879.
[13] T. Strother, T. Knickerbocker, J.N. Russell, J.E. Butler, L.M. Smith, R.J. Hamers, Langmuir 18 (2002) 968.
[14] T. Yamada, T.J. Chuang, H. Seki, Y. Mitsuda, Mol. Phys. 76 (1992) 887.
[15] G.J. Zhang, K.S. Song, Y. Nakamura, T. Ueno, T. Funatsu, I. Ohdomari, H. Kawarada, Langmuir 22 (2006) 3728.
[16] M. Nonnenmacher, M.P. O'Boyle, H.K. Wickramasinghe, Appl. Phys. Lett. 58 (1991) 2921.
[17] M. Tachiki, Y. Kaibara, Y. Sumikawa, M. Shigeno, T. Banno, K.S. Song, H. Umezawa, H. Kawarada1, Phys. Status Solidi 199 (2003) 39.
[18] B. Rezek, C.E. Nebel, Diamond Relat. Mater. 14 (2005) 466.
[19] B. Kaestner, C. Schönjahn, C.J. Humphreys, Appl. Phys. Lett. 84 (2004) 2109.
[20] M. Kudo, Y. Sakai, Appl. Phys. Lett. 76 (2000) 3475.
[21] A.P. Janssen, P. Akhtar, C.J. Harland, J.A. Venables, Surf. Sci. 93 (1980) 453.
[22] M.C. Salvadori, V.P. Mammana, O.G. Martins, F.T. Degasperi, Plasma Sources Sci. Technol. 4 (1995) 489.
[23] M.A. Brewer, I.G. Brown, M.R. Dickinson, J.E. Galvin, R.A. MacGill, M.C. Salvadori, Rev. Sci. Instrum. 63 (1992) 3389.
[24] C. Popov, W. Kulisch, P.N. Gibson, G. Ceccone, M. Jelinek, Diamond Relat. Mater. 13 (2004) 1371.
[25] S. Orlanducci, A. Fiori, V. Sessa, E. Tamburri, F. Toschi, M.L. Terranova, J. Nanosci. Nanotechnol. 8 (2008) 3228.
[26] A.C. Ferrari, J. Robertson, Phys. Rev. B 64 (2001) 075414.
[27] R. Pfeiffer, H. Kuzmany, N. Salk, B. Günther, Appl. Phys. Lett. 82 (2003) 4149.
[28] F. Silva, F. Bénédic, P. Bruno, A. Gicquel, Diamond Relat. Mater. 14 (2005) 398.
[29] A. Vizir, E.M. Oks, M.C. Salvadori, F.S. Teixeira, I.G. Brown, Rev. Sci. Instrum. 78 (2007) 086103.
[30] A.S. Metel', Sov. Phys. Tech. Phys. 29 (1984) 141.
[31] N.V. Gavrilov, E.M. Oks, Nucl. Instrum. Methods Phys. Res., A 439 (2000) 31.
[32] N.V. Gavrilov, G.A. Mesyats, G.V. Radkovski, V.V. Bersenev, Surf. Coat. Technol. 96 (1997) 81.
[33] W.D. Deininger, G. Asyon, L.C. Pless, Rev. Sci. Instrum. 58 (1987) 1053.